ARTICLE

Theoretical Study on the Rotational Spectra of Ar-$D_2{}^{32}S$ Complex[†]

Jin-ping Lei, Yan-zi Zhou, Dai-qian Xie*

Institute of Theoretical and Computational Chemistry, Key Laboratory of Mesoscopic Chemistry, School of Chemistry and Chemical Engineering, Nanjing University, Nanjing 210093, China

(Dated: Received on October 30, 2013; Accepted on November 12, 2013)

We report a theoretical study on the rotational spectra of Ar-$D_2{}^{32}S$. The intermolecular potential energy surface was transformed from our latest *ab initio* three-dimensional potential of Ar-$H_2{}^{32}S$. The rotational energy levels and wavefunctions of the complex were calculated by using the radial discrete variable representation/angular finite basis representation method and the Lanczos algorithm. The calculated rotational transition frequencies and structural parameters were found to be in good agreement with the available experimental values.

Key words: Rotational spectrum, Van der Waals complex, Molecular structure

I. INTRODUCTION

Van der Waals (vdW) complexes between rare-gas (Rg) atoms and nonlinear H_2X (X=O, S) molecules have attracted considerable attention [1−7]. As an analogs of water, hydrogen sulfide (H_2S) is an interesting weak bonding partner, because sulfur itself is a key element in the spectroscopy of giant planets [8]. On the other hand, the studies of vdW complexes containing H_2S can be used to explore the differences in the H_2O analogs in terms of configuration and intermolecular dynamics [9]. Our theoretical study of the Ar-D_2S vdW complex was initiated by the observation of an unusual deuterium isotope effect in the microwave study of Ar-H_2S, Ar-D_2S, and Ar-HDS by Gutowsky *et al.* [10].

The spectroscopy of the weakly bound vdW complexes can provide useful information on the geometries and intermolecular dynamics of these molecules. However, only a few number of experimental information has been available for the Rg-H_2S complexes and mainly focused on the Ar-H_2S and Ne-H_2S complexes. The microwave spectra of Ar-H_2S and its isotopomers were reported by Viswanathan and Dyke [11], Bumgarner *et al.* [12], and Gutowsky *et al.* [10]. The rotational transitions were assigned, and the structural parameters and internal dynamics were also discussed. As discussed by Gutowsky *et al.* [10], as the deuterium substitution of H_2S, D_2S led to an unusual increase in the rotational constant of the lower state of Ar-H_2S, not the usual decrease as for the case of Ar-H_2O [10, 13]. Later in 2002, Liu and Jager reported the rotational spectra and internal dynamics for fifteen isotopomers of Ne-H_2S [14]. All the experimental studies revealed that these Rg-H_2S complexes are characterized by a planar equilibrium structure.

Theoretical studies on the rotational spectra of the vdW complexes could be employed to check the quality of the *ab initio* potential energy surfaces (PES) and provide complete description of the spectra. In our previous work, we have constructed an intermolecular potential energy surface (IPES) for the Ar-H_2S complex at CCSD(T) level with aug-cc-pVQZ basis set plus bond functions, and predicted the rotational bound states of this complex [15]. The calculated rotational transition frequencies and structural parameters of Ar-H_2S were in good agreement with the available experimental results.

In this work, we provide detailed information on the dynamics including the rotational energy levels, rotational transition frequencies, and structural parameters for Ar-$D_2{}^{32}S$. The calculated rotational transition frequencies and structural parameters were compared with the available experimental values.

II. COMPUTATIONAL DETAILS

The geometry of the Ar-D_2S complex is defined by the Jacobi coordinates: R, θ, and φ, as shown in Fig.1. R is the intermolecular distance between the D_2S center of mass and the argon atom, θ is the angle between the vector $\mathbf{R}$ and the C_2 axis of the D_2S monomer, and the dihedral angle φ denotes the out-of-plane rotation of the Ar atom related to the plane of D_2S. Based on the potential points for Ar-$H_2{}^{32}S$ of our previous work [15], we obtained the PES of Ar-$D_2{}^{32}S$ by transforming the center of mass coordinates from Ar-$D_2{}^{32}S$ to Ar-$H_2{}^{32}S$.

The intermolecular Hamiltonian of the Ar-D_2S com-

[†]Part of the special issue for "the Chinese Chemical Society's 13th National Chemical Dynamics Symposium".

*Author to whom correspondence should be addressed. E-mail: dqxie@nju.edu.cn

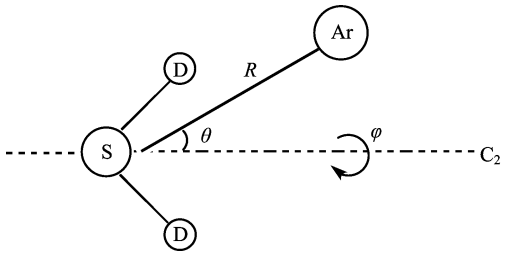

FIG. 1 Jacobi coordinates for the Ar-D_2S complex. R is the distance between the center of mass of D_2S and the Ar atom, θ denotes the angle between the vector $\mathbf{R}$ and C_2 axis of D_2S, and φ is the out of plane angle of the Ar atom rotating around the plane of D_2S. The reference frame is chosen at φ=0° when the four atoms are coplanar and θ=0° when Ar lies on the C_2 axis.

plex in the Jacobi coordinates can be written as (h=1),

$$\hat{H} = -\frac{1}{2\mu}\frac{\partial^2}{\partial R^2} + \frac{1}{2\mu R^2}(\hat{J}-\hat{j})^2 + \hat{H}_{\rm monomer} + V(R,\theta,\varphi) \quad (1)$$

where μ is the reduced mass of the Ar-D_2S complex. J and j are the angular momentum operators corresponding to overall and the D_2S monomer rotations, respectively. V is the intermolecular potential energy of the complex. The D_2S monomer Hamiltonian $H_{\rm monomer}$ is chosen as a standard Watson A-reduced Hamiltonian including the effects of the quadric centrifugal distortions [4, 16],

$$\begin{aligned} H_{\rm monomer} &= \left(\frac{A+C}{2}\right)\hat{j}^2 + \left[B-\left(\frac{A+C}{2}\right)\right]\hat{j}_z^2 + \\ &\left(\frac{A-C}{4}\right)(\hat{j}_+^2+\hat{j}_-^2) - \Delta_j\hat{j}^4 - \Delta_k\hat{j}_z^4 - \\ &\Delta_{jk}\hat{j}^2\hat{j}_z^2 - 2\delta_j\hat{j}^2(\hat{j}_+^2+\hat{j}_-^2) - \\ &\delta_k[\hat{j}_z^2(\hat{j}_+^2+\hat{j}_-^2)+(\hat{j}_+^2+\hat{j}_-^2)\hat{j}_z^2] \end{aligned} \quad (2)$$

here the rotational constants (A, B, and C) and the quadric centrifugal distortion coefficients (Δ_j, Δ_k, Δ_{jk}, δ_j, and δ_k) for D_2S were taken from the experimental data [17].

The intermolecular stretching mode for the R coordinate is represented by sine DVR [18]. For the angular part, we used the parity-adapted rotational basis function $\Theta_{jk}^{JMK\varepsilon}$ in the following form [4],

$$\begin{aligned} \Theta_{jk}^{JMK\varepsilon} &= \frac{1}{\sqrt{2(1+\delta_{K0}\delta_{k0})}}[D_{MK}^{J^*}(\alpha,\beta,\gamma)\cdot \\ &D_{Kk}^{j^*}(0,\theta,\varphi)+\varepsilon(-1)^{J+k}\cdot \\ &D_{M-K}^{J^*}(\alpha,\beta,\gamma)D_{-K-k}^{j^*}(0,\theta,\varphi)] \end{aligned} \quad (3)$$

where ε is the space-inversion parity, M is the projection of the total angular momentum J on the z-axis of space-fixed frame, K is the projection of both J and j on the body-fixed (BF) z-axis, and k is the projection of j on the z-axis of the molecule H_2S fixed frame. $D_{MK}^{J^*}(\alpha,\beta,\gamma)$ is the normalized rotational function for the overall rotation of the complex, and $D_{Kk}^{j^*}(0,\theta,\varphi)$ is the rotational function which describes the rotation of the D_2S monomer. The Lanczos method [19, 20] was employed to diagonalize the Hamiltonian matrix to produce the energy levels and eigenfunctions.

TABLE I The rotational energy levels for the Ar-D_2S and Ar-H_2S complexes on the $\Sigma(0_{00})$ and $\Sigma(1_{01})$ states (in cm^{-1}).

J	$\Sigma(0_{00})$ state		$\Sigma(1_{01})$ state	
	Ar-$D_2{}^{32}S$	Ar-$H_2{}^{32}S$	Ar-$D_2{}^{32}S$	Ar-$H_2{}^{32}S$ [15]
0	−117.282	−111.553	−116.377	−104.611
1	−117.170	−111.443	−116.265	−104.498
2	−116.946	−111.223	−116.040	−104.271
3	−116.610	−110.892	−115.702	−103.932
4	−116.162	−110.452	−115.252	−103.479
5	−115.602	−109.901	−114.690	−102.913
6	−114.931	−109.241	−114.015	−102.234

III. ROTATIONAL BOUND STATES AND TRANSITION FREQUENCIES

The rotational energy levels for the Ar-D_2S complex were calculated by the radial DVR/angular FBR method [21−23] and Lanczos algorithm [19, 24]. In our calculations, we used 80 sine DVR grid points for the R coordinate ranging from 4.5 a_0 to 22.0 a_0. For the angular coordinates, we applied $n_\theta \times n_\varphi$=24×24 DVR grid points and 12 basis functions for θ. The calculated energy levels were found to be converged to 0.001 cm^{-1} or better. The rotational bound states of Ar-D_2S are assigned by the notation "$nK(j_{k_a k_c})$" following the scheme proposed by Hutson [25] and Cohen *et al.* [16, 26]. n denotes the intermolecular stretching mode (typically we omit it when n=0). K is the projection of J on the z-axis of BF frame, and states with K=0, 1, 2, ... are labeled by the Greek capital letters Σ, Π, Δ, ..., and $j_{k_a k_c}$ describes the rotational states of the D_2S monomer. The rotational wavefunctions of the D_2S monomer conserve its symmetry relative to the BF z-axis, so the parity constraint is given by $(-1)^k=(-1)^{k_a+k_c}$.

Table I lists the rotational energies of the lowest two states $\Sigma(0_{00})$ and $\Sigma(1_{01})$ with J up to 6 of Ar-$D_2{}^{32}S$ and Ar-$H_2{}^{32}S$ complexes for comparison. The rotational energy for the ground state $\Sigma(0_{00})$ of Ar-$D_2{}^{32}S$ is found to be −117.282 cm^{-1}, indicating that the zero-point energy is about 60.19 cm^{-1}, which is lower than that (65.9 cm^{-1}) of Ar-$H_2{}^{32}S$ [15]. The zero-point energy is significantly higher than the energy barrier height (47.37 cm^{-1}), which means that the ground $\Sigma(0_{00})$ state

DOI:10.1063/1674-0068/26/06/656-660

TABLE II Comparison between observed and calculated transition frequencies of the Ar-$D_2{}^{32}S$ comlex on the $\Sigma(0_{00})$ and $\Sigma(1_{01})$ states (in cm^{-1}).

	$\Sigma(0_{00})$ state			$\Sigma(1_{01})$ state		
J'-J''	Expt.[10]	Calc.	Diff.	Expt.[12]	Calc.	Diff.
1-0	0.114	0.112	−0.002	0.114	0.112	−0.002
2-1		0.224		0.228	0.225	−0.003
3-2		0.336		0.341	0.338	−0.003
4-3		0.448		0.455	0.450	−0.005
5-4		0.560		0.569	0.562	−0.007
6-5		0.671			0.675	

spreads over the global minimum, similar to the case of Ar-$H_2{}^{32}S$ [15]. The first excited intermolecular vibrational state $\Sigma(1_{01})$ lies 0.9 cm^{-1} above the ground state and is relative to the first rotational state of D_2S monomer in the complex. It is clear from Table I that the rotational energy levels for the Ar-$D_2{}^{32}S$ complex are lower than that for Ar-$H_2{}^{32}S$, due to the heavier mass of the D_2S subunit which leads to the increase of the reduced mass of the Ar-$D_2{}^{32}S$ complex. Besides, our calculated transition frequencies from J=0 to J=1 for the ground $\Sigma(0_{00})$ state of the Ar-$D_2{}^{32}S$ complex is a little higher than that for the Ar-$H_2{}^{32}S$ complex (0.112 cm^{-1} versus 0.110 cm^{-1}), indicating that our calculated rotational constant for the Ar-$D_2{}^{32}S$ complex is larger than that for the Ar-$H_2{}^{32}S$ complex, the same as the experimental results [10].

The rotational transition frequencies for the $\Sigma(0_{00})$ and $\Sigma(1_{01})$ states of the Ar-$D_2{}^{32}S$ complex were calculated and compared with the available experimental results [10−12]. The calculated results are given in Table II together with the avaiable experimental values. It is apparent that our calculated transition frequencies are in good accordance with the observed values with the deviations within 0.01 cm^{-1}. Good agreement between the calculated and observed rotational transition frequencies demonstrates the high quality of our potential.

IV. STRUCTURE CHARACTERISTICS

The theoretical averaged structural parameters $\bar{R}$, $\bar{\theta}$, and $\bar{\varphi}$ were determined from the ground state wavefunctions of the complex with the following equations [4, 27],

$$\frac{1}{\bar{R}^2} = \langle\psi|\frac{1}{R^2}|\psi\rangle \tag{4}$$

$$\cos\bar{\theta} = \langle\psi|\cos\theta|\psi\rangle \tag{5}$$

$$\cos^2\bar{\varphi} = \langle\psi|\cos^2\varphi|\psi\rangle \tag{6}$$

The calculated average structures for the $\Sigma(0_{00})$ and $\Sigma(1_{01})$ states of Ar-$D_2{}^{32}S$ are listed in Table III together with the experimental estimated values [10, 12]. It is

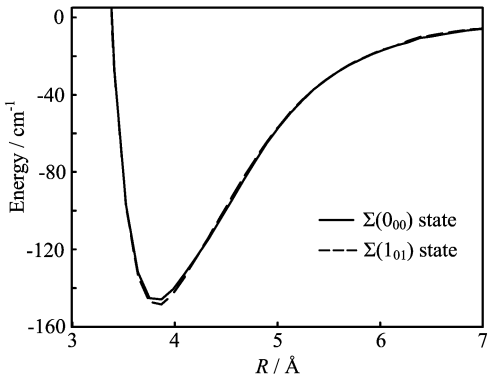

FIG. 2 The effective energy of the $\Sigma(0_{00})$ and $\Sigma(1_{01})$ states of Ar-$D_2{}^{32}S$ as a function of R.

TABLE III The average structural parameters of the Ar-$D_2{}^{32}S$ complex on the $\Sigma(0_{00})$ and $\Sigma(1_{01})$ states.

	$\Sigma(0_{00})$ state		$\Sigma(1_{01})$ state		
	Calc.	Expt.[10]	Calc.	Expt. [11]	Expt.[10]
$\bar{R}$/Å	3.979	3.821	3.952	3.921	3.795
$\bar{\theta}$/(°)	101.33		106.10	102.80	
$\bar{\varphi}$/(°)	26.04		21.71		

shown that the calculated values of $\bar{R}$ and $\bar{\theta}$ are in good accordance with the experimental values. The average intermolecular distance $\bar{R}$ for the ground rovibrational state $\Sigma(0_{00})$ is about 0.24 Å longer than its equilibrium value (3.979 Å versus 3.742 Å), considerably deviated from the global minimum structure of the potential, which demonstrates the large amplitude zero-point motion within the complex. $\bar{R}$ for the ground state $\Sigma(0_{00})$ of Ar-$D_2{}^{32}S$ is 3.979 Å, which is a little shorter than that of Ar-$H_2{}^{32}S$ (4.092 Å) [15], the same tendency of isotopic shift as the experimental results [10].

It is interesting that the value of $\bar{R}$ for the ground state $\Sigma(0_{00})$ is a little longer than that for the first excited state $\Sigma(1_{01})$, similar to the case of Ar-$H_2{}^{32}S$ [15] and Ar-H_2O [26]. In order to better understand the dynamic behavior of Ar-$D_2{}^{32}S$ on the two bound states as a function R, we plot the effective radial potentials in Fig.2 and the reduced one-dimensional probability densities in Fig.3. The effective radial potentials, which are obtained by averaging the potential over the angular coordinates θ and φ with the ground rovibrational wavefunctions, can manifest the effects of the anisotropy in the potential. As shown in Fig.2, the well depth on the effective radial potential energy curve for the $\Sigma(1_{01})$ state is about 2.56 cm^{-1} deeper than the $\Sigma(0_{00})$ state, and the value of R at the maximal probability density for the $\Sigma(1_{01})$ state is a little shorter than that for the $\Sigma(0_{00})$ state (Fig.3(a)). As a result, the $\Sigma(1_{01})$ state is less destabilized with higher barrier height and distributed closer to the global minimum, and it is reasonable that the calculated value of $\bar{R}$ for the $\Sigma(0_{00})$ state is longer than that for the $\Sigma(1_{01})$ state. Stabilization of

DOI:10.1063/1674-0068/26/06/656-660

the j=1 internal rotor levels has also been reported for Ne-H_2S [28], Ar-H_2S [15], Ar-H_2O [26], and some other complexes containing H_2, such as H_2-HF [29, 30] and H_2-stilbene [31].

The properties of the probability densities can also help to understand the relevant dynamic information of the complex. The reduced one-dimensional probability densities along two angular coordinates θ and φ are presented in Fig.3. As can be seen from Fig.3(b), the distribution of θ for the $\Sigma(0_{00})$ state is more dispersive, while the distribution for the $\Sigma(1_{01})$ state is significant around the global minimum. This shows that the amplitude of internal rotational motion of the D_2S monomer in the ground $\Sigma(0_{00})$ state is lager than that in the $\Sigma(1_{01})$ state, so that the calculated value of $\bar{\theta}$ for the $\Sigma(1_{01})$ state is closer to the structure of global minimum than that for the $\Sigma(0_{00})$ state. On the other hand, Fig.3(c) illustrates that the out-of-plane rotation becomes more difficult for the $\Sigma(1_{01})$ state than that for the $\Sigma(0_{00})$ state, and the D_2S subunit is more restricted near the global minimum for the $\Sigma(1_{01})$ state than for the $\Sigma(0_{00})$ state. This indicates that the internal rotation of D_2S for the $\Sigma(0_{00})$ state is more free than that for the $\Sigma(1_{01})$ state. Therefore, the first excited state $\Sigma(1_{01})$ deviates more from free rotation limit of D_2S monomer than the ground $\Sigma(0_{00})$ state. All these dynamic properties are similar to that for the Ar-H_2S complex in our previous work [15].

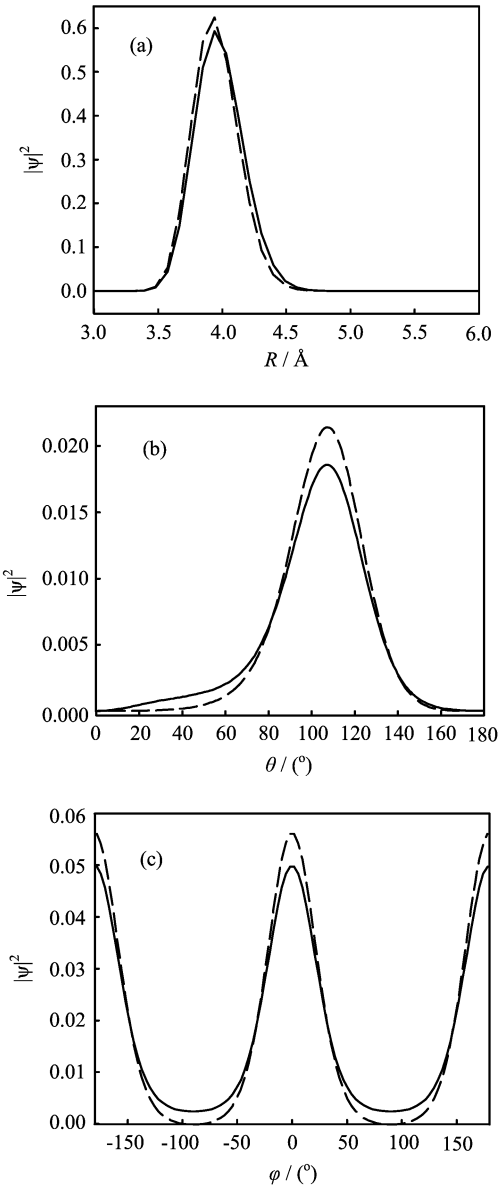

FIG. 3 The reduced one-dimensional probability densities of the $\Sigma(0_{00})$ (solid lines) and $\Sigma(1_{01})$ (broken lines) states of Ar-$D_2{}^{32}S$ as functions of (a) R, (b) θ, and (c) φ.

V. CONCLUSION

We have presented the theoretical study for the rotational spectra of Ar-$D_2{}^{32}S$. The intermolecular potential energy surface was transformed from our latest *ab initio* three-dimensional potential of Ar-$H_2{}^{32}S$. The bound rotational energy levels of the Ar-D_2S complex were obtained by employing the radial DVR/angular FBR method and Lanczos algorithm. The calculated rotational transition frequencies and structural parameters are in reasonable agreement with the available experimental values.

VI. ACKNOWLEDGMENTS

This work was supported by the National Natural Science Foundation of China (No.20273066, No.91021010, and No.21273104).

[1] P. R. P. Barreto, F. Palazzetti, G. Grossi, A. Lombardi, G. S. Maciel, and A. F. A. Vilela, Int. J. Quantum. Chem. **110**, 777 (2010).
[2] S. Li, R. Zheng, Y. Zhu, and C. X. Duan, J. Chem. Phys. **135**, 134304 (2011).
[3] A. Haskopoulos and G. Maroulis, J. Phys. Chem. A **114**, 8730 (2010).
[4] L. Wang and M. H. Yang, J. Chem. Phys. **129**, 174305 (2008).
[5] Q. Wen and W. Jager, J. Phys. Chem. A. **110**, 7560 (2006).
[6] D. Cappelletti, A. F. A. Vilela, P. R. P. Barreto, R. Gargano, F. Pirani, and V. Aquilanti, J. Chem. Phys. **125**, 133111 (2006).
[7] J. Makarewicz, J. Chem. Phys. **129**, 184310 (2008).
[8] J. M. Flaud, C. Camy-Peyret, and J. W. C. Johns, Can. J. Phys. **61**, 1462 (1983).
[9] Y. J. Xu, P. Arboleda, and W. Jager, J. Mol. Spectrosc. **229**, 47 (2005).
[10] H. S. Gutowsky, T. Emilsson, and E. Arunan, J. Chem.

DOI:10.1063/1674-0068/26/06/656-660

Phys. **106**, 5309 (1997).
[11] R. Viswanathan and T. R. Dyke, J. Chem. Phys. **82**, 1674 (1985).
[12] R. E. Bumgarner, D. J. Pauley, and S. G. Kukolich, J. Mol. Struct. **190**, 163 (1988).
[13] G. de Oliveira and C. E. Dykstra, J. Chem. Phys. **106**, 5316 (1997).
[14] Y. Q. Liu and W. Jager, Mol. Phys. **100**, 611 (2002).
[15] J. P. Lei, Y. Z. Zhou, and D. Q. Xie, J. Chem. Phys. **136**, 084310 (2012).
[16] R. C. Cohen and R. J. Saykally, J. Chem. Phys. **98**, 6007 (1993).
[17] R. L. Cook, F. C. Delucia, and P. Helminger, J. Mol. Struct. **28**, 237 (1975).
[18] D. T. Colbert and W. H. Miller, J. Chem. Phys. **96**, 1982 (1992).
[19] C. Lanczos, J. Res. Natl. Bur. Stand. **45**, 255 (1950).
[20] H. Guo, R. Q. Chen, and D. Q. Xie, J. Theor. Comput. Chem. **1**, 173 (2002).
[21] S. Y. Lin and H. Guo, J. Chem. Phys. **117**, 5183 (2002).
[22] R. Q. Chen, G. B. Ma, and H. Guo, Chem. Phys. Lett. **320**, 567 (2000).
[23] C. Leforestier, J. Chem. Phys. **101**, 7357 (1994).
[24] C. C. Paige, J. Inst. Math. Appl. **10**, 373 (1972).
[25] J. M. Hutson, J. Chem. Phys. **92**, 157 (1990).
[26] R. C. Cohen, K. L. Busarow, Y. T. Lee, and R. J. Saykally, J. Chem. Phys. **92**, 169 (1990).
[27] R. C. Cohen and R. J. Saykally, J. Phys. Chem. **94**, 7991 (1990).
[28] J. P. Lei, M. Y. Xiao, Y. Z. Zhou, and D. Q. Xie, J. Chem. Phys. **136**, 214307 (2012).
[29] C. M. Lovejoy, D. D. Nelson, and D. J. Nesbitt, J. Chem. Phys. **87**, 5621 (1987).
[30] C. M. Lovejoy, D. D. Nelson, and D. J. Nesbitt, J. Chem. Phys. **89**, 7180 (1988).
[31] D. O. Dehaan and T. S. Zwier, J. Chem. Phys. **90**, 1460 (1989).

DOI:10.1063/1674-0068/26/06/656-660